# Inclusion compounds of a diol host with xylidines: controlled stoichiometries

**Luigi R. Nassimbeni\* and
Hong Su**

Department of Chemistry, University of Cape Town, Rondebosch 7701, South Africa

Correspondence e-mail:
xrayluig@science.uct.ac.za

The diol host, 1,1′-bis-(4-hydroxyphenyl)cyclohexane (DHPC) and a number of xylidine isomers as guests formed a series of inclusion compounds that gave rise to various host:guest ratios controlled by crystallization temperatures. For the host DHPC with a particular xylidine isomer, the number of guests included generally decreases as the crystallization temperature increases. The crystal structures of these host–guest compounds were elucidated using single-crystal X-ray diffraction. Their thermal stabilities were characterized by TG and DSC analysis. The selectivity of enclathration by the host was measured by carrying out a series of competition experiments. The kinetics of guest decomposition were studied using isothermal and non-isothermal methods and reconciled with the crystal structures.

## 1. Introduction

The stoichiometry of inclusion compounds is determined by their topology. Thus, the number of guest molecules that are entrapped by a given host is dependent on whether the host geometry gives rise to layers (intercalates), channels (tubulates), pockets (aediculates) or cages (cryptates). This forms the basis for the classification and nomenclature of host–guest compounds (Weber & Josel, 1983).

An important parameter for controlling the host:guest ratio is the crystallization temperature. Previous reports of this phenomenon include the two compounds of *trans*-3,3′-bis(diphenylhydroxymethyl)azobenzene with acetone, which yields a host:guest ratio of 1:2 when crystallized at room temperature, but forms a different compound of 1:1 stoichiometry when the former compound is melted and cooled to 353.2 K under reduced pressure (Hamada *et al.*, 1992). Varying the crystallization temperature has been used to control the selectivity of xylene isomers by binaphthyl dicarboxylic acid (Beketov *et al.*, 1999) and to change the host:guest ratio of the inclusion compounds formed between an alicyclic diol and 1,2-dichlorobenzene (Ung *et al.*, 1993). In general, the number of guest molecules entrapped by a host will decrease with increasing crystallization temperature, but in the case of binaphthyldicarboxylic acid with DMSO the host:guest ratio changes from 1:1 to 1:2 when the crystallization temperature is raised from 323 to 333 K. Disorder in both the host and guest molecules is apparent in these structures and is an important factor in the formation of the clathrates (Makhkamov *et al.*, 1999). The inclusion compounds formed between binaphthol and 1,4-dioxane at different temperatures have been described, their thermal characteristics and kinetics of desolvation have been measured (Nassimbeni & Su, 2000). General rules on how topology is likely to change with crys-

tallization temperature have been formulated (Ibragimov, 1999).

We now present structural results for the clathrates obtained between the host 1,1'-bis-(4-hydroxyphenyl)cyclohexane (DHPC) and a number of xylidine isomers as guests, some of which were crystallized at different temperatures. The thermal stabilities of the compounds as well as the guest selectivities are discussed. The atomic numbering scheme, host:guest ratios, crystallization temperatures and compound code names are shown below.
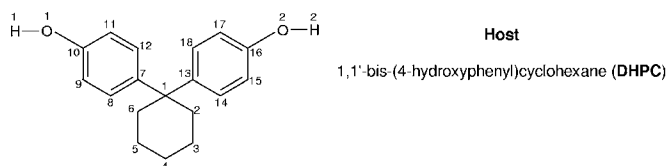


| | Guest | Host:guest | Crystallisation temperature | Code name |
|---|---|---|---|---|
| | 2,6-Xylidine | 1:1 | 80°C | DC26X1 |
| | (26X) | 1:1.5 | 25, 60°C | DC26X1.5 |
| | | 1:2.5 | 4°C | DC26X2.5 |
| | | 1:3 | 1°C | DC26X3 |
| | 2,3-Xylidine | 1:0.5 | 80°C | DC23X0.5 |
| | (23X) | 1:2 | 25°C | DC23X2 |
| | 3,4-Xylidine | 1:0.5:1H$_2$O | 25°C (in toluene) | DC34X0.5 |
| | (34X) | 1:1 | 80°C | DC34X1 |
| | 3,5-Xylidine | 1:1 | 25°C | DC35X1 |
| | (35X) | | | |

## 2. Experimental

### 2.1. Syntheses

The inclusion compounds were obtained by dissolving the host compound DHPC in the liquid xylidines and crystals of suitable quality appeared by slow evaporation within periods varying between 24 h and 7 d. Where crystallization was carried out at elevated temperatures, the glass vials containing the solutions were placed in brass blocks, which were placed in heated sand baths. The temperatures were controlled to within ±1 K. Low-temperature crystallization was carried out in refrigerators set at ±277 and ±274 K, respectively. In the case of 3,4-xylidine, which is solid at ambient temperature, toluene was used as a non-competitive solvent for the crystallization carried out at 298 K.

### 2.2. Data collection, structure solution and refinement

Preliminary cell dimensions and space group symmetry were determined photographically and subsequently refined on a Nonius Kappa CCD diffractometer using graphite-monochromated Mo $K\alpha$ radiation. The strategy for the data collections was evaluated using the *COLLECT* software, and scaled and reduced with *DENZO-SMN* (Otwinowski & Minor, 1997). All structures were solved by direct methods using *SHELX*86 (Sheldrick, 1985) and refined by full-matrix least-squares on $F^2$ with *SHELX*97 (Sheldrick, 1997). Diagrams were prepared with the aid of *X-seed* (Barbour, 1999). Salient crystal and experimental data for all structures are given in Table 1.[1] The hydrogen-bonding details for all the structures are given in Table 2.

For all the structures, direct methods yielded the positions of all the non-H atoms, which were subsequently refined with anisotropical displacement parameters. The hydroxyl H atoms on the host and the amino H atoms on the guest were located in difference electron-density maps and refined with simple bond-length constraints and independent isotropic temperature factors. The other H atoms were placed with geometrical constraints and refined with isotropic temperature factors assigned as either 1.2 or 1.5 times the value of the $U_{eq}$ of their parent atoms. In the structures of DC26X1, DC26X1.5 and DC23X0.5, the guest molecules were disordered, as discussed below. In the structure of DC23X0.5, each hydroxyl group of the host is bifurcated due to the disordered guest molecule to which it is hydrogen bonded, and the hydrogen was located over two sites with occupancy factor 0.5. In the structure of DC23X2, one of the methyl groups was modelled using six H atom sites with occupancy 0.5, offset from one another by 60° rotations.

### 2.3. Competition experiments

These were carried out between pairs of guests by preparing a number of host–guest solutions, systematically changing the mole fractions of one guest. The ensuing crystals were filtered and the guest mixture was analysed by gas chromatography. These experiments were extended to analyse simultaneous competition by three xylidine isomers. Competition between 2,3-xylidine and 3,4-xylidine was not carried out because they could not be separated. Further experimental details on this technique have appeared recently (Nassimbeni & Su, 2001).

### 2.4. Thermal analysis and kinetics of desolvation

Thermogravimetry (TG) and differential scanning calorimetry (DSC) were carried out on a Perkin-Elmer PC7-Series system. The TG and DSC experiments were performed over the temperature range 303–503 K, at a heating rate of 10 K min$^{-1}$ with a purge of dry nitrogen flowing at 30 ml min$^{-1}$. The samples were crushed, blotted dry and placed in open platinum pans for TG experiments and in crimped but vented aluminium pans for DSC. Data for the

---

[1] Supplementary data for this paper are available from the IUCr electronic archives (Reference: AN0588). Services for accessing these data are described at the back of the journal.

**Table 1**
Experimental details.

| | DC26X1 | DC26X1.5 | DC26X3 | DC23X0.5 | DC23X2 |
|---|---|---|---|---|---|
| **Crystal data** | | | | | |
| Chemical formula | $C_{18}H_{20}O_2 \cdot C_8H_{11}N$ | $C_{18}H_{20}O_2 \cdot 1.5C_8H_{11}N$ | $C_{18}H_{20}O_2 \cdot 3C_8H_{11}N$ | $C_{18}H_{20}O_2 \cdot 0.5C_8H_{11}N$ | $C_{18}H_{20}O_2 \cdot 2C_8H_{11}N$ |
| Chemical formula weight | 389.52 | 450.11 | 631.87 | 328.93 | 510.7 |
| Cell setting, space group | Triclinic, $P\bar{1}$ | Triclinic, $P\bar{1}$ | Monoclinic, $P2_1/n$ | Monoclinic, $C2/c$ | Triclinic, $P\bar{1}$ |
| $a, b, c$ (Å) | 6.234 (1), 10.934 (2), 16.974 (2) | 7.8594 (3), 10.015 (1), 17.169 (1) | 9.807 (1), 25.464 (2), 29.842 (3) | 18.1704 (10), 12.2744 (10), 16.2036 (10) | 6.3593 (3), 10.8368 (5), 21.7366 (11) |
| $\alpha, \beta, \gamma$ (°) | 84.98 (1), 81.29 (2), 77.10 (2) | 78.909 (2), 85.161 (1), 71.238 (1) | 90, 98.28 (1), 90 | 90, 95.30 (2), 90 | 93.429 (3), 91.100 (3), 106.912 (3) |
| $V$ (Å$^3$) | 1113.1 (3) | 1255.33 (15) | 7374.6 (12) | 3598.5 (4) | 1429.57 (12) |
| $Z$ | 2 | 2 | 8 | 8 | 2 |
| $D_x$ (Mg m$^{-3}$) | 1.162 | 1.191 | 1.138 | 1.214 | 1.186 |
| Radiation type | Mo $K\alpha$ | Mo $K\alpha$ | Mo $K\alpha$ | Mo $K\alpha$ | Mo $K\alpha$ |
| $\mu$ (mm$^{-1}$) | 0.072 | 0.074 | 0.069 | 0.076 | 0.073 |
| Temperature (K) | 293 (2) | 173 (2) | 173 (2) | 173 (2) | 173 (2) |
| Crystal form, colour | Prism, colourless | Prism, colourless | Prism, colourless | Cuboid, colourless | Prism, colourless |
| Crystal size (mm) | $0.40 \times 0.30 \times 0.25$ | $0.50 \times 0.35 \times 0.15$ | $0.80 \times 0.50 \times 0.20$ | $0.40 \times 0.40 \times 0.30$ | $0.50 \times 0.40 \times 0.30$ |
| **Data collection** | | | | | |
| Diffractometer | Nonius Kappa CCD | Nonius Kappa CCD | Nonius Kappa CCD | Nonius Kappa CCD | Nonius Kappa CCD |
| Data collection method | $1°$ $\varphi$ and $\omega$ scans | $1°$ $\varphi$ and $\omega$ scans | $0.8°$ $\varphi$ and $\omega$ scans | $1°$ $\varphi$ and $\omega$ scans | $1°$ $\varphi$ and $\omega$ scans |
| No. of measured, independent and observed parameters | 4040, 3895, 2435 | 6193, 4593, 2742 | 13 682, 13 682, 8177 | 9719, 3283, 2558 | 6145, 4517, 3292 |
| Criterion for observed reflections | $I > 2\sigma(I)$ | $I > 2\sigma(I)$ | $I > 2\sigma(I)$ | $I > 2\sigma(I)$ | $I > 2\sigma(I)$ |
| $R_{int}$ | 0.0179 | 0.0172 | 0.070 | 0.0215 | 0.0175 |
| $\theta_{max}$ (°) | 24.97 | 25.64 | 25.68 | 25.34 | 26.26 |
| Range of $h, k, l$ | $0 \rightarrow h \rightarrow 7$ | $-6 \rightarrow h \rightarrow 9$ | $0 \rightarrow h \rightarrow 11$ | $-21 \rightarrow h \rightarrow 20$ | $-7 \rightarrow h \rightarrow 7$ |
| | $-12 \rightarrow k \rightarrow 12$ | $-12 \rightarrow k \rightarrow 11$ | $0 \rightarrow k \rightarrow 30$ | $-14 \rightarrow k \rightarrow 13$ | $-13 \rightarrow k \rightarrow 13$ |
| | $-19 \rightarrow l \rightarrow 20$ | $-20 \rightarrow l \rightarrow 20$ | $-36 \rightarrow l \rightarrow 35$ | $-19 \rightarrow l \rightarrow 17$ | $-26 \rightarrow l \rightarrow 22$ |
| **Refinement** | | | | | |
| Refinement on | $F^2$ | $F^2$ | $F^2$ | $F^2$ | $F^2$ |
| $R[F^2>2\sigma(F^2)]$, $wR(F^2)$, $S$ | 0.0557, 0.1849, 1.091 | 0.056, 0.1487, 1.038 | 0.0862, 0.2338, 1.059 | 0.0349, 0.0904, 1.052 | 0.0448, 0.12, 1.027 |
| No. of reflections and parameters used in refinement | 3895, 347 | 4593, 344 | 13 682, 923 | 3283, 288 | 4517, 371 |
| H-atom treatment | Mixed | Mixed | Mixed | Mixed | Mixed |
| Weighting scheme | $w = 1/[\sigma^2(F_o^2) + (0.0670P)^2 + 0.7169P]$, where $P = (F_o^2 + 2F_c^2)/3$ | $w = 1/[\sigma^2(F_o^2) + (0.0734P)^2 + 0.0396P]$, where $P = (F_o^2 + 2F_c^2)/3$ | $w = 1/[\sigma^2(F_o^2) + (0.0896P)^2 + 7.8821P]$, where $P = (F_o^2 + 2F_c^2)/3$ | $w = 1/[\sigma^2(F_o^2) + (0.0402P)^2 + 1.4007P]$, where $P = (F_o^2 + 2F_c^2)/3$ | $w = 1/[\sigma^2(F_o^2) + (0.0553P)^2 + 0.3573P]$, where $P = (F_o^2 + 2F_c^2)/3$ |
| $(\Delta/\sigma)_{max}$ | 0.112 | 0.000 | 0.023 | 0.010 | 0.000 |
| $\Delta\rho_{max}$, $\Delta\rho_{min}$ (e Å$^{-3}$) | 0.779, $-0.171$ | 0.418, $-0.183$ | 0.627, $-0.251$ | 0.176, $-0.155$ | 0.208, $-0.176$ |
| Extinction method | *SHELXL* | *SHELXL* | *SHELXL* | *SHELXL* | *SHELXL* |
| Extinction coefficient | 0.026 (4) | 0.014 (3) | 0.0003 (5) | 0.0027 (3) | 0.021 (2) |

| | DC34X0.5 | DC34X1 | DC35X1 |
|---|---|---|---|
| **Crystal data** | | | |
| Chemical formula | $C_{18}H_{20}O_2 \cdot 0.5C_8H_{11}N \cdot H_2O$ | $C_{18}H_{20}O_2 \cdot C_8H_{11}N$ | $C_{18}H_{20}O_2 \cdot C_8H_{11}N$ |
| Chemical formula weight | 346.95 | 389.52 | 389.52 |
| Cell setting, space group | Triclinic, $P\bar{1}$ | Monoclinic, $C2/c$ | Triclinic, $P\bar{1}$ |
| $a, b, c$ (Å) | 10.8979 (5), 12.5017 (7), 15.1701 (7) | 34.965 (1), 6.2546 (3), 20.2035 (8) | 6.327 (1), 10.720 (2), 16.920 (4) |
| $\alpha, \beta, \gamma$ (°) | 106.510 (4), 99.895 (3), 102.559 (2) | 90, 101.577 (1), 90 | 96.481 (15), 100.094 (17), 99.827 (14) |
| $V$ (Å$^3$) | 1872.93 (16) | 4328.5 (3) | 1101.1 (4) |
| $Z$ | 4 | 8 | 2 |
| $D_x$ (Mg m$^{-3}$) | 1.230 | 1.195 | 1.175 |
| Radiation type | Mo $K\alpha$ | Mo $K\alpha$ | Mo $K\alpha$ |
| $\mu$ (mm$^{-1}$) | 0.081 | 0.074 | 0.073 |
| Temperature (K) | 173 (2) | 173 (2) | 293 (2) |
| Crystal form, colour | Prism, colourless | Prism, colourless | Prism, colourless |
| Crystal size (mm) | $0.30 \times 0.30 \times 0.20$ | $0.35 \times 0.25 \times 0.20$ | $0.40 \times 0.40 \times 0.30$ |
| **Data collection** | | | |
| Diffractometer | Nonius Kappa CCD | Nonius Kappa CCD | Nonius Kappa CCD |

**Table 1** (continued)

| | DC34X0.5 | DC34X1 | DC35X1 |
|---|---|---|---|
| Data collection method | $1°\varphi$ scans and $\omega$ scans | $0.8°\varphi$ scans and $\omega$ scans | $1°\varphi$ scans and $\omega$ scans |
| No. of measured, independent and observed parameters | 10 118, 6720, 3621 | 7707, 4699, 2949 | 4014, 3869, 2067 |
| Criterion for observed reflections | $I > 2\sigma(I)$ | $I > 2\sigma(I)$ | $I > 2\sigma(I)$ |
| $R_{int}$ | 0.0215 | 0.1107 | 0.0392 |
| $\theta_{max}$ (°) | 25.42 | 28.24 | 24.97 |
| Range of $h, k, l$ | $-13 \rightarrow h \rightarrow 11$ | $-43 \rightarrow h \rightarrow 44$ | $0 \rightarrow h \rightarrow 7$ |
| | $-11 \rightarrow k \rightarrow 15$ | $-4 \rightarrow k \rightarrow 8$ | $-12 \rightarrow k \rightarrow 12$ |
| | $-18 \rightarrow l \rightarrow 15$ | $-25 \rightarrow l \rightarrow 25$ | $-20 \rightarrow l \rightarrow 19$ |
| | | | |
| Refinement | | | |
| Refinement on | $F^2$ | $F^2$ | $F^2$ |
| $R[F^2>2\sigma(F^2)]$, $wR(F^2)$, $S$ | 0.0654, 0.1487, 1.031 | 0.1043, 0.2823, 1.157 | 0.0439, 0.1374, 1.109 |
| No. of reflections and parameters used in refinement | 6720, 497 | 4699, 278 | 3869, 281 |
| H-atom treatment | Mixed | Mixed | Mixed |
| Weighting scheme | $w = 1/[\sigma^2(F_o^2) + (0.0322P)^2 + 2.1868P]$, where $P = (F_o^2 + 2F_c^2)/3$ | $w = 1/[\sigma^2(F_o^2) + (0.0000P)^2 + 16.4095P]$, where $P = (F_o^2 + 2F_c^2)/3$ | $w = 1/[\sigma^2(F_o^2) + (0.0323P)^2 + 0.4445P]$, where $P = (F_o^2 + 2F_c^2)/3$ |
| $(\Delta/\sigma)_{max}$ | 0.000 | 0.000 | 0.000 |
| $\Delta\rho_{max}$, $\Delta\rho_{min}$ (e Å$^{-3}$) | 0.379, −0.364 | 0.393, −0.295 | 0.202, −0.176 |
| Extinction method | $SHELXL$ | $SHELXL$ | $SHELXL$ |
| Extinction coefficient | 0.0027 (6) | 0.0043 (8) | 0.038 (3) |

Computer programs used: *COLLECT*, *DENZO-SMN* (Otwinowski & Minor, 1997), *SHELXL*97 (Sheldrick, 1997).

isothermal kinetics of desolvation were obtained from TG at selected temperatures. Non-isothermal kinetic studies were carried out using TG running at different heating rates.

## 3. Results and discussion

### 3.1. Structures

DC26X1 crystallizes in $P\bar{1}$ with $Z = 2$ and therefore both host and guest molecules are in general positions. The structure is characterized by columns of host···host molecules running along [010], stabilized by host···host (O—H···O) hydrogen bonds and a second column of host···guest···host molecules running along [100], displaying O—H···N—H···O—H··· hydrogen bonds. This is shown in Fig. 1(a). The metrics of the hydrogen bonds are given in Table 2. The guest molecules are disordered (Fig. 1b) and were refined with anisotropic displacement parameters and final site occupancies of 0.521 and 0.479. The packing is characterized by layers of host and guest molecules perpendicular to [001], as shown in Fig. 1(c), while the projection along [100] (Fig. 1d) shows the columns of hydrogen bonds which spiral in the [100] direction and link the layers of host and guest molecules.

DC26X1.5 crystallizes in $P\bar{1}$ with $Z = 2$ and therefore contains two host and three guest molecules in the unit cell. One guest molecule is therefore located at a centre of inversion at Wyckoff position (e) and is disordered. This is shown in Fig. 2(a). The hydrogen bonding is such that two host molecules form a dimer about a centre of inversion via (host)O—H···O(host) interactions and, in addition, are hydrogen bonded to the guest molecules. This is shown in Fig. 2(b). The

packing is characterized by layers of host and guest molecules similar to that of DC26X1.

DC26X2.5 is triclinic, space group $P\bar{1}$ with $Z = 4$. We failed to solve this structure fully, despite carrying out three complete data collections on different crystals at low temperature. On each attempt the refinement yielded sensible positions for the atoms of the host molecules and three of the five guest molecules in the asymmetric unit. However, the remaining two guest molecules proved intractable and gave unreasonable geometries. The final $R$ factor of 0.187 was clearly unsatisfactory and we therefore report only the unit-cell parameters for this compound [$C_{18}H_{20}O_2 \cdot 2.5C_8H_{11}N$, $M_r = 571.29$, triclinic, space group $P\bar{1}$, $a = 7.885$ (1), $b = 10.026$ (1), $c = 43.761$ (3) Å, $\alpha = 94.661$ (1), $\beta = 91.539$ (2), $\gamma = 109.020$ (1)°, $V = 3254.6$ (6) Å$^3$, $Z = 4$].

DC26X3 crystallizes in $P2_1/c$ with $Z = 8$ and there were two host and six guest molecules located in the asymmetric unit. The structure is characterized by columns of guest molecules running parallel to [401] at $y = 0$ and 1/2, and another column of guests running along [$\bar{1}$01] at $y = 1/4$ and 3/4. An example is given in Fig. 3(a). The packing is shown in Fig. 3(b). The host molecules are not hydrogen bonded to each other, two of the guests (molecules $B$ and $D$, Fig. 3b) are also not hydrogen bonded and details of the other hydrogen bonds are given in Table 2.

DC23X0.5 crystallizes in the space group $C2/c$ with $Z = 8$. The four guest molecules are therefore disordered about the diads at Wyckoff position (e), as shown in Fig. 4(a). The disordered guests are found in cavities centred at $y \simeq 1/3$. This is shown in Fig. 4(b). The structure is stabilized by (host)O—H···O(host) and (host)O—H···N(guest) hydrogen bonds, running along two directions, [100] and [010]. The packing is

shown in Fig. 4(*c*), in which the hydrogen bonds are shown by dotted lines.

DC23X2 crystallizes in $P\bar{1}$ ($Z = 2$) with one host and two guest molecules in the asymmetric unit. The packing is characterized by definite alternating layers of host and guest molecules perpendicular to [001], as shown in Fig. 5. The host···host, host···guest, guest···host and guest···guest hydrogen bonds link the host and the guest molecules in both the [100] and [010] directions.

DC34X0.5 is triclinic, $P\bar{1}$ with $Z = 4$. We located two hosts, one guest and two water molecules in general positions. The structure is characterized by layers of host molecules and guest–water molecules. The water molecules act as a hydrogen-bonding bridge between hosts and guests, as shown in Fig. 6.

DC34X1 crystallizes in $C2/c$ ($Z = 8$) with one host and one guest molecule in the asymmetric unit, both located in general positions. The structure has layers perpendicular to [100] and the hydrogen bonds link the host and guest molecules in a column of host···guest···host molecules, stabilized by hydrogen bonds O—H···N—H···O—H···, similar to the pattern exhibited by DC26X1.

DC35X1 crystallizes in $P\bar{1}$ ($Z = 2$) with one host and one guest molecule in the asymmetric unit, both in general positions. The structure is similar to that of DC26X1, in that the packing again exhibits layers of host and guest molecules perpendicular to [001]. The guest, however, is not disordered and the hydrogen bonding follows the same pattern of host···guest and host···guest···host running in the [010] and [100] directions, respectively.



**Figure 1**
Diagrams for the structure of DC26X1. (*a*) Part of the structure showing the hydrogen-bonding scheme. All the H atoms except the hydroxyl and amino hydrogens are omitted and the O and N atoms are shown as solid circles. The hydrogen bonds are shown as dotted lines. (*b*) Disorder modelled for the 2,6-xylidine molecule. (*c*) Space-filling diagram along [010] showing the alternative layers of the hosts and guests. The host molecules are shown in van der Waals radii and the guest molecules are shown as in (*a*), with the H atoms omitted. (*d*) Projection along [100] showing the crystal packing. Details as in (*a*).

### 3.2. Competition experiments

The results of the competition experiments are shown in Fig. 7. Each two-component experiment shows the mole fractions $X$ of a given guest in the initial mixture solution *versus* the mole fractions $Z$ of that guest included by the host. We note that 3,5-xylidine is preferentially enclathrated over 2,6-xylidine (Fig. 7*a*). 2,3-Xylidine is preferred to 2,6-xylidine, but not to 3,5-xylidine which gives a concentration-dependant result (Fig. 7*b*). 3,4-Xylidine is selected preferentially to 2,6-xylidine and, mostly, over 3,5-xylidine (Fig. 7*c*). We also carried out a series of three-component competition experiments, as shown in Fig. 7(*d*). The results are displayed as equilateral triangles in which the apices represent a pure component, the black dots give the composition of the starting mixtures and the result are given by the arrows. For the 26X/34X/35X system, the 3,4-xylidine is nearly always the preferred isomer. For the 26X/35X/23X system, 3,5-xylidine is preferred for all mixtures for which the initial mole fraction $X_{35X}$ is greater than 0.2, otherwise 2,3-xylidine is enriched. In no case is 2,6-xylidine the preferred isomer.

We have carried out the lattice energy calculation using the program *MPA* (Williams, 1999), as described previously (Nassimbeni & Su, 2001). We are aware that comparative values of the lattice energies are only strictly valid between host–guest systems of
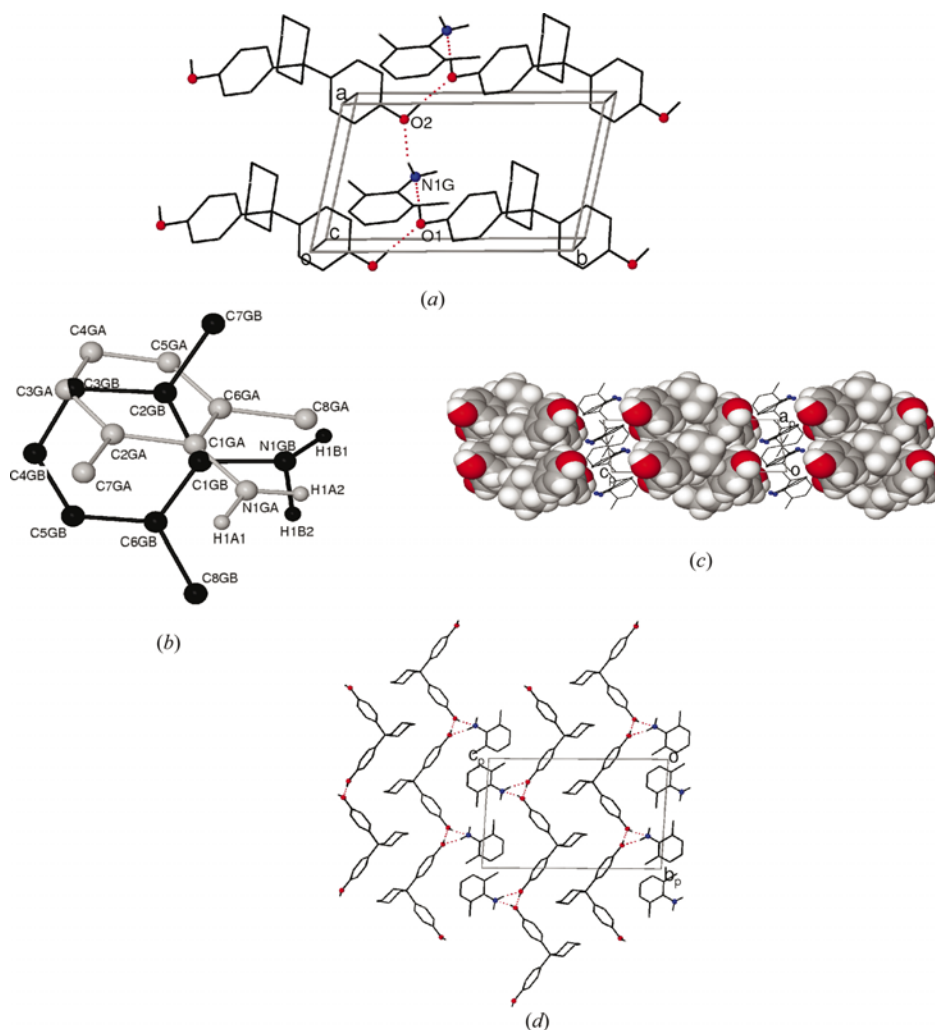
**Table 2**
Details of hydrogen bonding for the structures of the inclusion compounds.

| | $D$—H$\cdots A$ | H$\cdots A$ (Å) | $D\cdots A$ (Å) | <DHA (°) |
|---|---|---|---|---|
| DC26X1 | O1—H1$\cdots$N1$GA$ | 1.97 (3) | 2.896 (7) | 160 (4) |
| | N1$GA$—H1$A2\cdots$O2$^{i}$ | 2.28 (3) | 3.209 (7) | 162 (9) |
| | O2—H2$\cdots$O1$^{ii}$ | 1.78 (3) | 2.757 (3) | 172 (5) |
| | O1—H1$\cdots$N1$GB$ | 1.77 (3) | 2.642 (6) | 148 (4) |
| | N1$GB$—H1$B2\cdots$O2$^{i}$ | 2.29 (3) | 3.060 (6) | 136 (4) |
| DC26X1.5 | O1—H1$\cdots$N1$GA$ | 1.85 (1) | 2.804 (3) | 170 (3) |
| | O2—H2$\cdots$O1$^{iii}$ | 1.81 (1) | 2.758 (2) | 161 (3) |
| | N1$GA$—H1$A1\cdots$N1$GB$ | 2.51 (2) | 3.392 (3) | 154 (3) |
| | N1$GB\cdots$O2$^{iii}$ | – | 3.191 (3) | – |
| DC26X3 | O1$X$—H1$X\cdots$N1$GA^{iv}$ | 1.83 (2) | 2.781 (4) | 174 (4) |
| | O2$X$—H2$X\cdots$N1$GE$ | 1.93 (2) | 2.835 (4) | 171 (5) |
| | O1$Y$—H1$Y\cdots$N1$GC^{v}$ | 1.92 (2) | 2.819 (4) | 159 (4) |
| | O2$Y$—H2$Y\cdots$N1$GF^{v}$ | 1.87 (2) | 2.801 (4) | 166 (5) |
| | N1$GA$—H1$A2\cdots$O1$X^{vi}$ | 2.13 (3) | 3.025 (4) | 161 (4) |
| | N1$GC$—H1$C2\cdots$O2$Y^{vii}$ | 2.11 (2) | 3.042 (4) | 157 (3) |
| | N1$GE$—H1$E2\cdots$O2$X^{viii}$ | 2.24 (3) | 3.115 (4) | 155 (3) |
| | N1$GF$—H1$F2\cdots$O1$Y^{ix}$ | 2.24 (3) | 3.147 (4) | 165 (3) |
| DC23X0.5 | O1—H1$A\cdots$O2$^{x}$ | 1.71 (1) | 2.668 (1) | 178 (3) |
| | O1—H1$B\cdots$O1$^{xi}$ | 1.75 (1) | 2.700 (2) | 176 (5) |
| | O2—H2$A\cdots$N1$G^{xii}$ | 1.73 (2) | 2.689 (4) | 162 (3) |
| | O2—H2$B\cdots$O1$^{xiii}$ | 1.78 (2) | 2.668 (1) | 153 (3) |
| DC23X2 | O1—H1$\cdots$O2$^{ii}$ | 1.73 (1) | 2.707 (2) | 178 (2) |
| | O2—H2$\cdots$N1$GA^{xiv}$ | 1.76 (1) | 2.734 (2) | 172 (2) |
| | N1$GA$—H1$A2\cdots$O1 | 2.10 (1) | 3.033 (2) | 163 (2) |
| | N1$GA$—H1$A1\cdots$N1$GB$ | 2.98 (1) | 3.789 (3) | 146 (2) |
| DC34X0.5 | O1$X$—H1$X\cdots$O2$X^{iv}$ | 1.74 (1) | 2.709 (3) | 168 (3) |
| | O2$X$—H2$X\cdots$O1$W^{xv}$ | 1.67 (1) | 2.628 (4) | 172 (4) |
| | O1$Y$—H1$Y\cdots$O2$W^{xv}$ | 1.70 (2) | 2.651 (4) | 165 (4) |
| | O2$Y$—H2$Y\cdots$O1$Y^{iv}$ | 1.73 (1) | 2.688 (4) | 176 (4) |
| | O1$W$—H1$W1\cdots$O2$Y^{ii}$ | 1.82 (3) | 2.757 (4) | 173 (4) |
| | O1$W$—H1$W2\cdots$O2$W^{xvi}$ | 1.80 (3) | 2.740 (4) | 175 (4) |
| | O2$W$—H2$W1\cdots$O1$X$ | 1.83 (2) | 2.765 (4) | 161 (4) |
| | O2$W$—H2$W2\cdots$N1$G$ | 1.95 (2) | 2.923 (8) | 171 (3) |
| DC34X1 | O1—H1$\cdots$O2$^{xvii}$ | 1.77 (2) | 2.706 (4) | 166 (4) |
| | O2—H2$\cdots$N1$G^{xviii}$ | 1.78 (2) | 2.744 (5) | 173 (5) |
| | N1$G$—H1$G1\cdots$O1 | 2.02 (2) | 2.975 (5) | 166 (3) |
| DC35X1 | O2—H2$\cdots$N1$G^{xix}$ | 1.72 (1) | 2.697 (3) | 176 (4) |
| | O1—H1$\cdots$O2$^{xx}$ | 1.74 (1) | 2.701 (3) | 171 (3) |
| | N1$G$—H1$G1\cdots$O1$^{xxi}$ | 2.07 (2) | 3.013 (4) | 165 (3) |

Symmetry codes: (i) $x+1, y-1, z$; (ii) $x, y+1, z$; (iii) $-x+2, -y+1, -z+1$; (iv) $x-1, y, z$; (v) $x-1, y+1, z$; (vi) $-x+1, -y+1, -z$; (vii) $-x+\frac{1}{2}, y-\frac{1}{2}, -z+\frac{1}{2}$; (viii) $-x, -y+2, -z$; (ix) $-x+\frac{1}{2}, y-\frac{3}{2}, -z+\frac{1}{2}$; (x) $x+\frac{1}{2}, y-\frac{1}{2}, z$; (xi) $-x, y, -z+\frac{1}{2}$; (xii) $x-\frac{1}{2}, -y+\frac{1}{2}, z+\frac{1}{2}$; (xiii) $x-\frac{1}{2}, y+\frac{1}{2}, z$; (xiv) $x-1, y-1, z$; (xv) $x+1, y, z$; (xvi) $-x, -y+1, -z$; (xvii) $x, -y+2, z-\frac{1}{2}$; (xviii) $x, -y+1, z+\frac{1}{2}$; (xix) $-x+1, -y+1, -z+1$; (xx) $x, y-1, z$; (xxi) $-x, -y, -z+1$.

**Table 3**
Thermal analysis (TG/DSC) results.

| | Guest loss temperature ranges (°C) | Observed wt loss (%) | Calculated wt loss (%) | Guest loss onset temperature (°C) |
|---|---|---|---|---|
| DC26X1 | 66–158 | 30.2 | 31.11 | 92.4 |
| DC26X1.5 | 50–142 | 40.4 | 40.38 | 90.5 |
| DC26X2.5 | 40–146 | 52.9 | 53.03 | 88.0 |
| DC26X3 | 40–100 | 56.8 | 57.53 | N/A |
| DC23X0.5 | 110–186 | 18.1 | 18.42 | 139.8 |
| DC23X2 | 35–162 | 47.2 | 47.46 | 73.4 |
| DC34X0.5 | 42–162 | 22.5 | 22.66 | 86.2 |
| | | | | 119.6 |
| | | | | 130.2 |
| DC34X1 | 105–180 | 28.8 | 31.11 | N/A |
| DC35X1 | 130–188 | 28.1 | 31.11 | 124.2 |

the same host with guests which are isomers and where the host:guest ratios are identical. We therefore carried out the appropriate summation for the host$\cdots$host, host$\cdots$guest and
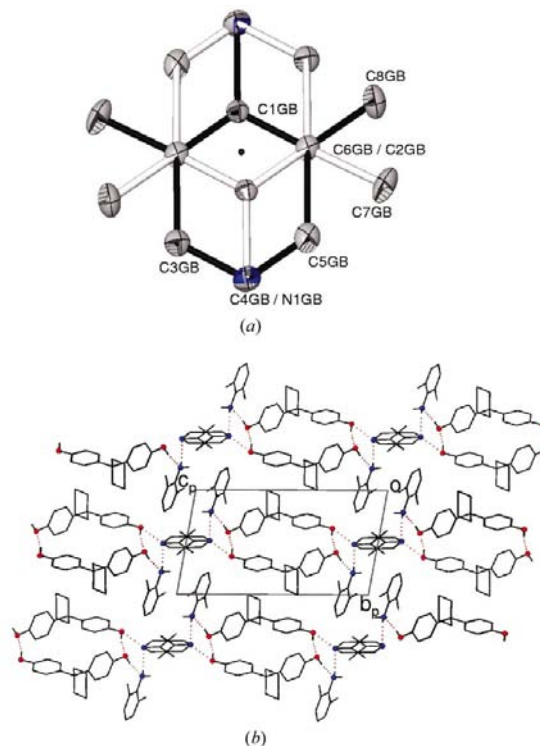


**Figure 2**
Structure diagrams for DC26X1.5. (*a*) Disorder modelled in the 2,6-xylidine molecule. (*b*) A projection down [100] showing the crystal packing. The artwork details are as in Fig. 1(*a*).
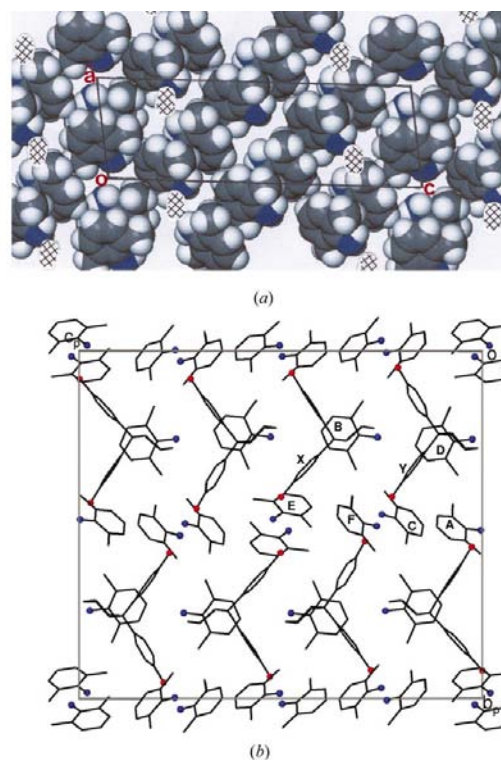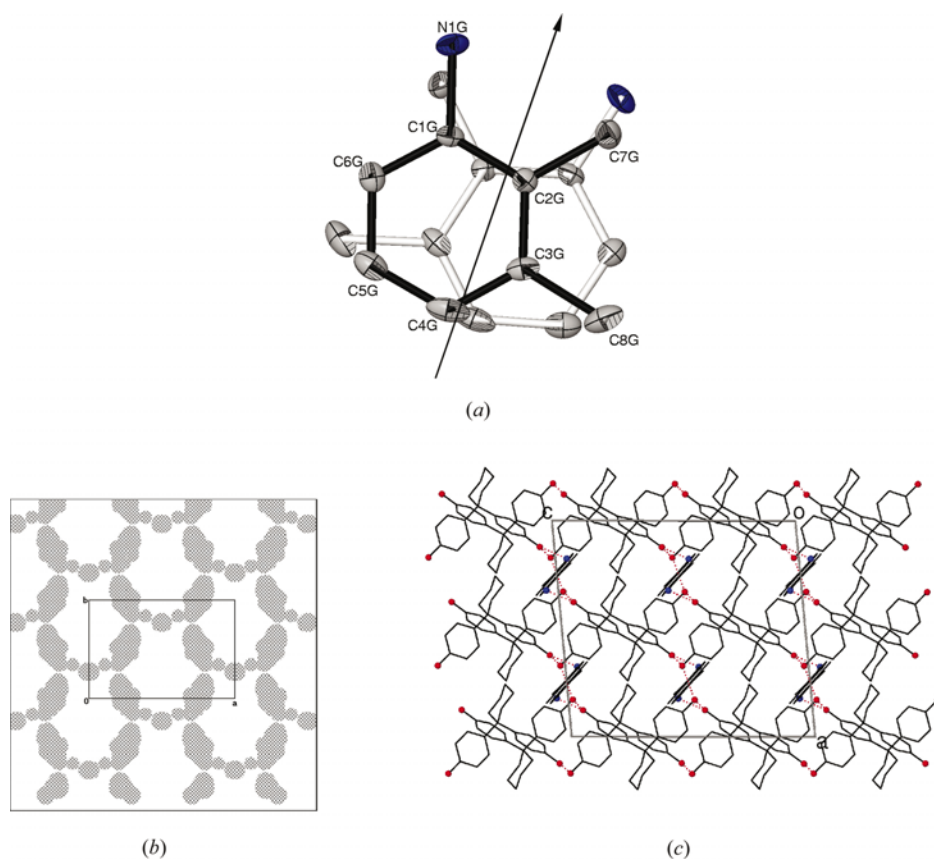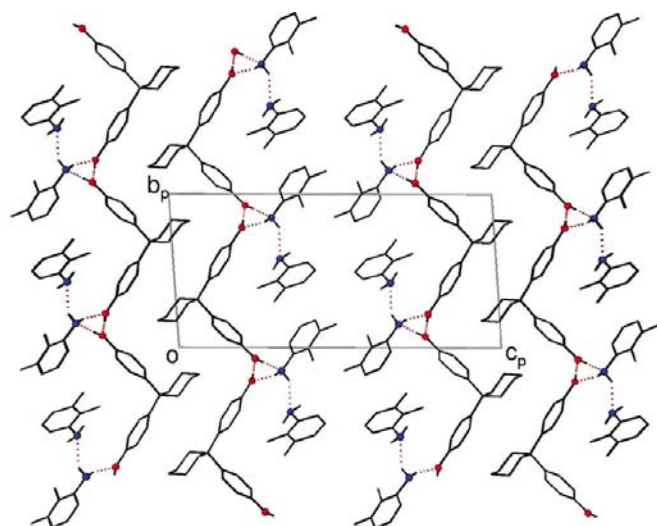


**Figure 3**
Diagrams for the structure of DC26X3. (*a*) A projection viewed down [010], with the diagonal crossed area representing the host cut at $y = 0$, showing the columns of guest molecules running along [401]. The guest molecules are shown with van der Waals radii. (*b*) A projection viewed down [100] showing the crystal packing. All the H atoms are omitted for clarity. The other details are as given in Fig. 1(*a*).

*(a)*



*(b)*



*(c)*

**Figure 4**
Diagrams for the structure of DC34X0.5. (*a*) Disorder modelled in the 3,4-xylidine molecule. (*b*) A cross section of the host framework cut at $z = 1/4$, showing the cavities where the guest molecules are located. The guest molecules are all omitted. (*c*) A projection viewed down [010] showing the crystal packing. All the H atoms are omitted for clarity. The other details are as given in Fig. 1(*d*).

guest···guest interactions for the compounds DC26X1, DC34X1 and DC35X1, which yielded −74.8, −181.9 and −173.8 kJ mol⁻¹. This is a gratifying result, showing that 2,6-

xylidine will always be disfavoured with respect to 3,4-xylidine and 3,5-xylidine. The latter two guests have similar lattice energies and give rise to concentration-dependent selectivity, as shown in Fig. 7(*c*), while Fig. 7(*d*) shows that 2,6-xylidine is never preferred.
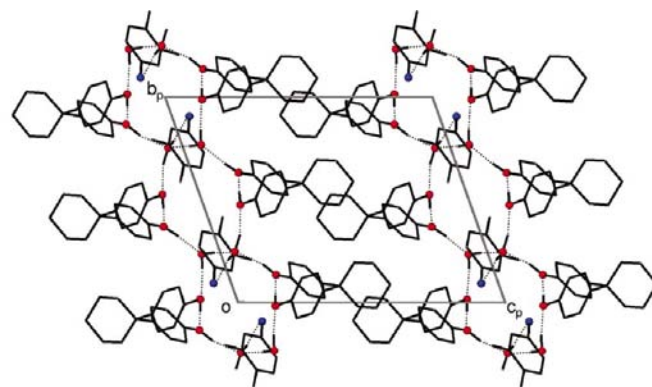
### 3.3. Thermal analysis and kinetics

The results of the TG analysis for DHPC·*n*(2,6-xylidine) are shown in Fig. 8(*a*). The TG traces show that the total mass losses correspond reasonably with the required stiochiometries of the host:guest ratios. The exact values are reported in Table 3 for all the structures discussed. Fig. 8(*b*) shows the TG/DSC traces for DC34X0.5. The desorption occurs in two steps, 4.9% loss corresponds to the desorption of water and is associated with endotherm *A*. The 3,4-xylidine desorption (17.6% weight loss) exhibits two endotherms *B* and *C*, while endotherm *D* is associated with the melt of the host compound. The other compounds exhibited simpler TG/DSC traces and the onset temperatures of desorption and mass losses are reported in Table 3.

We have analysed the kinetics of desolvation of DC35X1 and DC23X2. For DC35X1 we carried out a series of isothermal TG runs at selected temperatures between 338 and 388 K. The curves of the extent of reaction ($\alpha$) *versus* time (*t*) were deceleratory and were best fitted to the contracting area kinetic model R2 (Brown, 1988)

$$1 - (1 - \alpha)^{1/2} = kt.$$



**Figure 5**
A projection down [100] showing the crystal packing of DC34X2. Details are as given in Fig. 1(*a*).



**Figure 6**
A projection down [100] showing the crystal packing of DC34X0.5. Details are as given in Fig. 1(*a*).

The Arrhenius plot of ln $k$ *versus* $1/T$ is shown in Fig. 9 and yields values of 108 (5) kJ mol$^{-1}$ and 32 (2) min$^{-1}$ for the activation energy and the logarithm of the pre-exponential factor $A$, respectively.

DC23X2 decomposed in multiple steps and therefore the isothermal temperature method of analysis is not suitable. We therefore carried out a series of thermal decompositions at different heating rates (Flynn & Wall, 1966) and plotted the logarithm of the heating rate ($\beta$) *versus* $1/T$ for various percentage decompositions. The results are shown in Fig. 10, which yields activation energies varying from 64 (6) to 75 (6) kJ mol$^{-1}$.

## 4. Conclusions

The crystallizations of a series of the diol host DHPC with xylidines at various temperatures have yielded inclusion compounds with differing stoichiometries. The guest/host ratio decreases with increasing crystallization temperature, but in the case of 3,4-xylidine this pattern is broken by the incorporation of a water of crystallization. The topologies of the structures are generally characterized by layers of alternative host and guest molecules, but, interestingly, the high-temperature structure with 2,3-xylidine, with a low guest/host ratio of 0.5:1 (DC23X0.5), shows the guest to be entrapped in a definite cavity. All the structures are stabilized by a complex system of (host)O—H$\cdots$N(guest), (guest)N—H$\cdots$O(host), (guest)N—H$\cdots$N(guest) and (host)O—H$\cdots$O(host) hydrogen bonds. The kinetics of decomposition of DC23X2 and DC35X1 yield activation energies in the range 64–108 kJ mol$^{-1}$ and these relatively low values are justified by
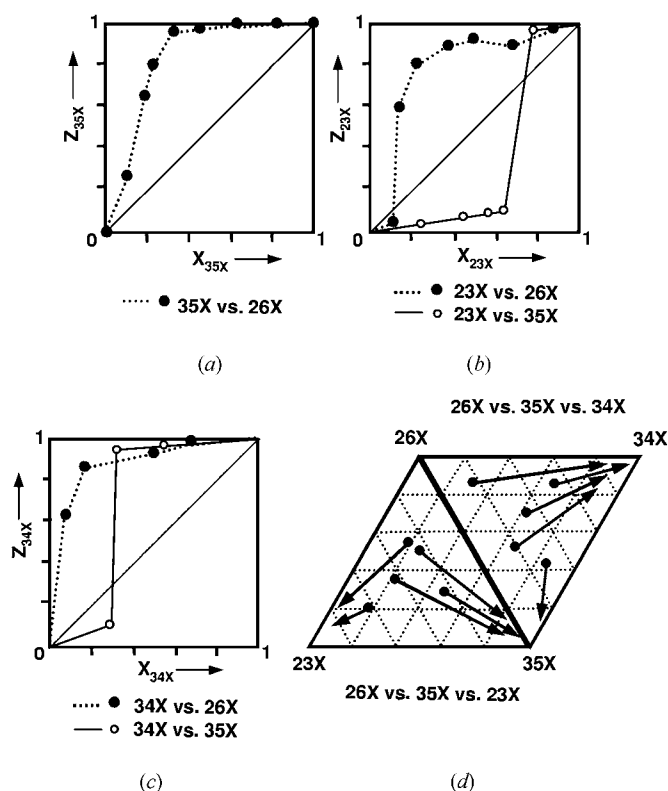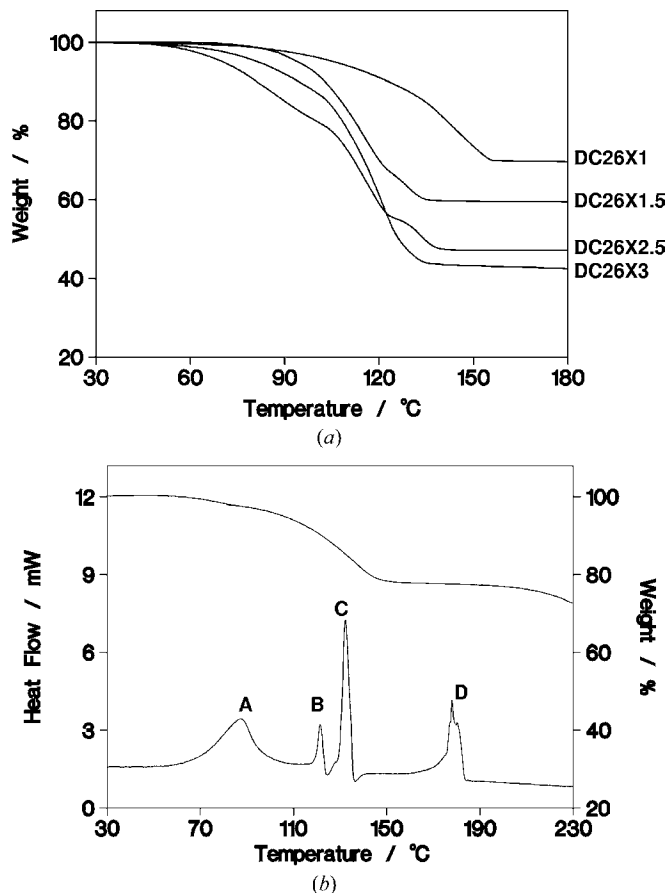


**Figure 8**
(*a*) TG traces for the DHPC·$n$(2,6-xylidine) inclusion compounds. (*b*) TG and DSC traces for DC34X0.5



**Figure 7**
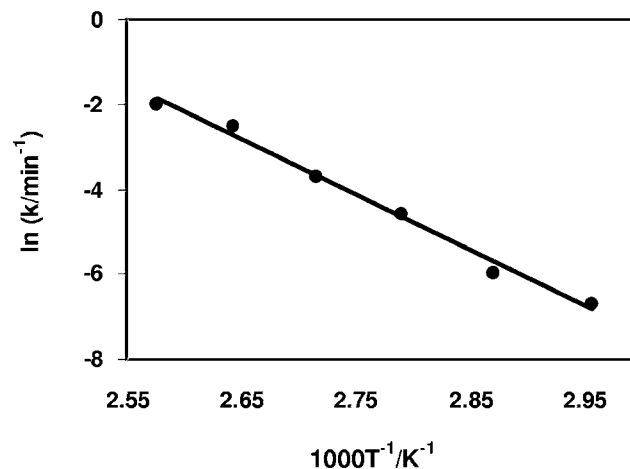Results of the competition experiments.



**Figure 9**
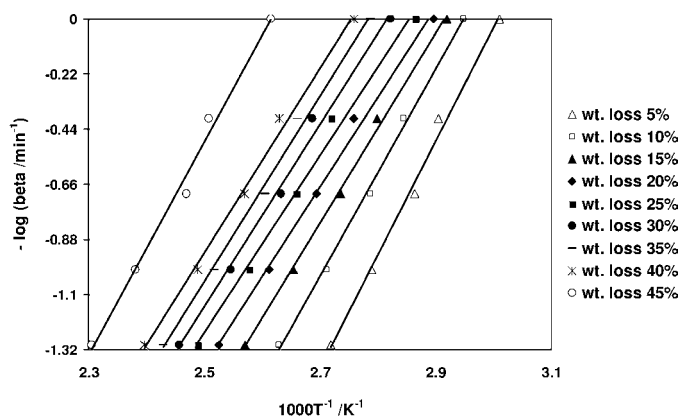Arrhenius plot of Ln $k$ *versus* $1/T$ for the decomposition of DC35X1.

**Figure 10**
Plots of $-\log \beta$ *versus* $1/T$ for the decomposition of DC23X2.

the open layer structures, which do not hinder the movement of guest molecules from the lattice.

## References

Barbour, L. J. (1999). *X-Seed.* University of Missouri–Columbia, USA.

Beketov, K., Weber, E., Seidel, J., Köhnke, K., Makhkamov, K. & Ibragimov, B. (1999). *Chem. Commun.* pp. 91–92.

Brown, M. E. (1988). *Introduction to Thermal Analysis – Techniques and Applications.* London: Chapman and Hall.

Flynn, J. H. & Wall, L. A. (1966). *Polym. Lett.* **4**, 323.

Hamada, K., Oh-hira, M., Fujiwara, T. & Toda, F. (1992). *Acta Cryst.* C**48**, 1969–1971.

Ibragimov, B. (1999). *J. Incl. Phenom. Macrocycl. Chem.* **34**, 345–353.

Makhkamov, K., Ibragimov, B. T., Weber, E. & Beketov, K. M. (1999). *J. Phys. Org. Chem.* **12**, 157–164.

Nassimbeni, L. R. & Su, H. (2000). *J. Phys. Org. Chem.* **13**, 368–371.

Nassimbeni, L. R. & Su, H. (2001). *Acta Cryst.* B**57**, 394–398.

Otwinowski, Z. & Minor, W. (1997). *Methods in Enzymology, Macromolecular Crystallography*, edited by C. W. Carter Jr & R. M. Sweet, Part A, Vol. 276, pp. 307–326. New York: Academic Press.

Sheldrick, G. M. (1985). *Crystallographic Computing*, edited by G. M. Sheldrick, C. Kruger & R. Goddard, Vol. 3, p. 175. Oxford University Press.

Sheldrick, G. M. (1997). *SHELX*97. University of Göttingen, Germany.

Ung, A. T., Bishop, R., Craig, D. C., Dance, I. G. & Scudder, M. L. (1993). *Tetrahedron*, **109**, 639–348.

Weber, E. & Josel, H.-P. (1983). *J. Incl. Phenom.* **1**, 79–85.

Williams, D. E. (1999). *MPA: Molecular Packing Analysis*, Version 2. Department of Chemistry, University of Louisville, Louisville, KY 40292, USA.